Sensitivity analysis of a strongly coupled aero-structural system using the discrete direct and adjoint methods

Meryem Marcelet* — Jacques Peter* — Gérald Carrier**

** ONERA - Department of Computational Fluid Dynamics and Aeroacoustics*
BP 72 - 29, avenue de la division Leclerc
F-92322 Châtillon cedex

meryem.marcelet@onera.fr, jacques.peter@onera.fr

*** ONERA - Applied Aerodynamics Department*
8, rue des Vertugadins
F-92190 Meudon

gerald.carrier@onera.fr

ABSTRACT. *This paper is dedicated to the sensitivity analysis of a static aeroelastic system with respect to design parameters governing its jig-shape. The gradients of interest are computed using either the discrete direct differentiation or adjoint vector methods. The aerodynamic load is predicted by the nonlinear Euler equations and transferred to the structure through a consistent and conservative procedure. The induced structural displacement field is computed using beam theory and the matrix of the aerodynamic influence coefficients. Finally, a threedimensional wing-body case is used to verify the successful implementation of the analytical sensitivity analysis methods.*

RÉSUMÉ. *Ce papier s'intéresse au calcul analytique des gradients d'un système aéroélastique statique par rapport à un vecteur de paramètres de forme. Les gradients sont calculés par les méthodes linéarisée ou adjointe discrètes. Les efforts aérodynamiques, prédits par les équations d'Euler non linéaires, sont transmis à la structure grâce à un processus consistant et conservatif. La théorie des poutres et l'approche matrice de flexibilité sont utilisées pour calculer le champ des déplacements de la structure. Ces méthodes sont finalement appliquées au calcul des gradients d'une configuration aile-fuselage tridimensionnelle.*

KEYWORDS: *shape optimization, sensitivity analysis, aeroelasticity, discrete direct differentiation method, discrete adjoint vector method.*

MOTS-CLÉS : *optimisation de forme, calcul de gradients, aéroélasticité, méthode linéarisée discrète, méthode adjointe discrète.*

DOI:10.3166/REMN.17.1077-1106

1. Introduction

Shape optimization is concerned with determining a set of design variables acting upon the shape of an object to be designed, so that an objective function is optimized while a set of constraints is satisfied. It appeared in the 70's when a group of engineers working for NASA first used computational fluid dynamic softwares within shape optimization processes (Hicks *et al.*, 1975; Hicks *et al.*, 1976a; Hicks *et al.*, 1976b; Vanderplaats *et al.*, 1976; Hicks *et al.*, 1977; Hicks *et al.*, 1978). The shapes they studied were simple (airfoil profile, wing plane shape...) and the fluid behavior was predicted by low-fidelity models (Pironneau, 1973). The optimal shape was determined according to gradient-based descent schemes relying on finite differencing for sensitivity calculation, and only the aerodynamic behavior was taken into account. In 1988, (Jameson, 1988) first introduced an analytical method for gradient computation inspired from optimal control theory (Lions, 1971) and called the adjoint vector method. Then in the early 90's, the direct differentiation method, another, more instinctive, analytical method for gradient computation, come out (Baysal *et al.*, 1991; Shubin, 1991; Burgreen *et al.*, 1996). Taking benefit from current growing computer capabilities, high-fidelity models have been used in conjunction with gradient computation analytical methods, on more and more complex geometries : for airfoil profiles first (Jameson, 1990; Jameson *et al.*, 1994), then on wing surfaces (Reuther, 1996; Jameson *et al.*, 1998), and finally on complete airplane geometries (Reuther *et al.*, 1996; Reuther *et al.*, 1999a; Reuther *et al.*, 1999b; Din *et al.*, 2006).

From a numerical point of view, shape optimization consists in chosing a discretized shape defined by its surface boundary mesh among a set of parametrized shapes. Numerical optimization enables the designer to conceive a shape which is not biased or limited by intuition or experience (or lack thereof). The constraint conditions must be satisfied in order for the design to be feasible. They can be explicitly used or incorporated in the objective function using penalty terms. Transforming the optimization problem into a minimization problem, finally consists in :

$$\text{finding } \alpha \text{ that minimizes } J(\alpha) \text{ subject to } \begin{cases} G(\alpha) \leq 0 \\ \alpha_{lb} \leq \alpha \leq \alpha_{ub} \end{cases}$$

where α is the vector of design variables, J is the objective, G is the vector of inequality constraints, α_{lb} and α_{ub} are the lower and upper bound vectors defining the design space to be explored.

NOTE. — a vector x of $\mathbb{R}^n$ satisfies $x \leq 0$ iff $\forall l \in [1, n], x_l \leq 0$.

The optimization problem can be tackled with two different famillies of methods (Vanderplaats, 1984). First, local algorithms, such as gradient-based algorithms and simplex method, search for an optimal shape in the neighborhood of an initial guess, usually close to a traditional designed-by-experience shape. Second, global algo-

rithms are intended to predict an absolute optimum in the design space. Most of them start from a set of shapes and make them evolve according to non-deterministic rules. If high-fidelity modeling is adopted (numerical flow computations for aerodynamics), they can turn out to be very expensive. In such cases, either lower fidelity physical models are chosen to predict design properties during the optimization process, or objective and constraints are partly replaced by surrogate models. However, neither of these two techniques is exclusive : global search can be used to locate areas of interest where local optimization can proceed. Examples of hybrid and sequential optimization techniques can be found in references (Carrier, 2004; Carrier, 2006).

Traditionally, only the aerodynamic behavior of the shape to be defined was taken into account during shape optimization and the design of complex multidisciplinary systems was performed sequentially *i.e.* in a loosely coupled sens. The different disciplines involved were treated separately by discipline experts trying to maximize their own performance-related criteria. For instance, the aerodynamic team was only concerned with designing a shape with minimum drag (shape optimization), while the structure team aimed at defining the characteristics of the structure so that it exhibits minimum structural weight and the propulsion team was interested in minimizing specific fuel consumption. However, Wakayama (Wakayama, 1994) has shown that sequential optimization does not necessarily converge to the true optimum of the multidisciplinary coupled system. Besides, engineering systems of practical interest are usually characterized by complex interactions between disciplines. Neglecting elastic deformations can result in overestimating aileron efficiency by 50% (Fillola *et al.*, 2004), or, as we have found for the DLR wing-fuselage F4 configuration, in overestimating lift and drag respectively by 10% and 20%. Furthermore, Arslan and Carlson (Arslan *et al.*, 1996) observed that sensitivity information produced by an aerodynamic-only calculation has different magnitude and in some case sign from that obtained with the coupled sensitivity analysis. Hence, the motivation for performing muldisciplinary analysis and optimization during the design process becomes obvious.

In this paper, the analytical framework that has been set up to compute the sensitivities required by the shape optimization of an aeroelastic system is presented. Section 2 introduces the different sensitivity computation methods, Section 3 describes the strongly coupled aeroelastic system we consider as well as the method implemented to solve for the static aeroelastic equilibrium, and at last, Section 4 derives the corresponding coupled systems of equations related to the discrete direct differentiation method and the discrete adjoint vector method. Finally, the discrete direct differentiation method and the discrete adjoint vector method are illustrated in Section 5 and the analytical sensitivity derivatives are compared to those predicted by the numerical finite differencing method.

2. Sensitivity calculations for a coupled system

Among every possible interactions between disciplines, aero-structural interaction is of primary importance for aeronautical applications. In the remainder of this paper, we will only concentrate on the sensitivity analysis of a strongly coupled aeroelastic system, sensitivity being a very useful information for design purpose, and essential for gradient-based optimization. In other words, flow properties and gradients required by local shape optimization techniques are computed based on coupled aero-structural system equations. The generic analytical framework for the sensitivity analysis of a strongly coupled system, influenced by the popular gradient-based methods used by the early structural optimization (Haug *et al.*, 1986; Kirsch, 1993; Bendsoe, 1995), was first introduced by Sobieszcsanski-Sobieski (Sobieszcsanski-Sobieski, 1990b; Sobieszcsanski-Sobieski, 1990a). In most aeroelastic sensitivity analyses, the structure is represented by a simple analytical model and the aerodynamic loads are evaluated by a linear theory (Haftka, 1986; Bowman *et al.*, 1989; Friedman, 1991; Barthelemy *et al.*, 1994). Nevertheless, for a dozen years, nonlinear aeroelastic cases have been considered, first for two-dimensional studies (Ghattas *et al.*, 1998; Moller *et al.*, 2002), then for three-dimensional cases (Giunta *et al.*, 1998; Giunta, 2000; Hou *et al.*, 2000; Maute *et al.*, 2001) considering only the direct differentiation approach, and recently using the adjoint method (Martins, 2000; Maute *et al.*, 2003; Fazzolari *et al.*, 2007). But, never has an analytical framework combining the influence matrix approach based on beam theory, for calculating the structure displacements, and Euler equations, for computing the fluid behavior, been presented for the analytical sensitivity analysis of a strongly coupled fluid-structure system. However, such a framework, which is presented in this paper, is particularly well-suited for preliminary design.

$$\frac{dJ}{d\alpha} = \frac{\partial J}{\partial \alpha} + \frac{\partial J}{\partial q}\frac{dq}{d\alpha} \qquad [1]$$

The system variables vector is denoted by q and its dimension by n_v. For the aeroelastic system, the global state variable vector will be defined as $q = (W, D)^T$ where W is the vector of the flow state variables, and D is the vector of structural displacements. The sensitivity analysis is concerned with assessing the gradients of a function J with respect to α. In the overall gradient-based optimization process, this function can be an objective or a constraint. The discrete set of the n_v governing equations is written in residual form as $R(\alpha, q) = 0$. The gradient of $J(\alpha, q(\alpha))$ with respect to α is given by Equation [1]. Since $R(\alpha, q(\alpha)) = 0$ is satisfied for every vector α, Equation [2] is satisfied.

$$\frac{dR}{d\alpha} = \frac{\partial R}{\partial \alpha} + \frac{\partial R}{\partial q}\frac{dq}{d\alpha} = 0 \Longrightarrow \frac{\partial R}{\partial q}\frac{dq}{d\alpha} = -\frac{\partial R}{\partial \alpha} \qquad [2]$$

Two different analytical approaches can be used to compute $dJ/d\alpha$. In the first approach, known as the direct differentiation approach, the sensitivity of the state variable vector with respect to α, $dq/d\alpha$, is computed by solving the direct differentia-

tion Equation [2], and then plugged back in Equation [1]. In the second approach, one uses Equation [3] (the superscript T designates the transpose of a vector or a matrix).

$$\forall \lambda \in \mathbb{R}^{n_v}, \quad \frac{dJ}{d\alpha} = \frac{\partial J}{\partial \alpha} + \frac{\partial J}{\partial q}\frac{dq}{d\alpha} + \lambda^T \left(\frac{\partial R}{\partial q}\frac{dq}{d\alpha} + \frac{\partial R}{\partial \alpha} \right) \quad [3]$$

The so-called adjoint vector λ, whose dimension is the same as the dimension of q and R, is chosen such that Equation [4] is satisfied. When the adjoint vector method is used, the designer does not compute the sensitivities of the state variables with respect to design parameters ($dq/d\alpha$) as he does when the direct differentiation approach is applied. Instead, he has to solve for the adjoint vector λ.

$$\left(\frac{\partial R}{\partial q} \right)^T \lambda = - \left(\frac{\partial J}{\partial q} \right)^T \quad [4]$$

This approach known as the adjoint vector method was first applied to aerodynamic sensitivities computation by (Jameson, 1988) but using the continuous form of the equations and then extended to the discrete equations (Shubin *et al.*, 1991; Baysal *et al.*, 1991). Both approaches require a set of linear systems to be solved. In the direct differentiation approach, n_α linear systems have to be solved, where n_α is the number of design parameters, as opposed to n_f in the adjoint approach, where n_f is the number of functions to differentiate (*i.e.* the objective function and the inequality constraint functions). Consequently, depending on whether $n_\alpha < n_f$ or $n_\alpha > n_f$ the direct differentiation or the adjoint approach is prefered.

Originally and up to the 90's, the gradient $dq/d\alpha$ required by the direct differentiation method was respectively first-order or second-order approximated by the popular finite differencing formula given by Equation [5].

$$\frac{dq}{d\alpha} \approx \frac{q(\alpha+\epsilon) - q(\alpha)}{\epsilon} + o(\epsilon) \approx \frac{q(\alpha+\epsilon) - q(\alpha-\epsilon)}{2\epsilon} + o(\epsilon^2) \quad [5]$$

The amplitude ϵ is empirically chosen and tuned according to the following procedure. Different values of ϵ are tested and the corresponding gradient approximation values are reported on a graph (versus ϵ). This process takes place till a stable zone is detected. The finite difference approach retains the corresponding constant value as the gradient approximation. Since the value of ϵ may be very small and since varying α may only induce small variations of q, it is important to evaluate every term using the double precision option for floats.

Compared to analytical methods, such as discrete direct differentiation and discrete adjoint vector methods, the finite difference approach is far more expensive in CPU as well as less accurate, which is the reason why analytical methods currently tend to supersede finite difference approximation techniques for gradient computations. Indeed, numerical sensitivity analysis requires at least $n_\alpha + 1$ state-variables

computations (solutions of nonlinear systems) versus one state-variables computation plus n_α (if the direct differentiation method is used) or n_f (if the adjoint method is used) solutions of linear systems for the analytical sensitivity analysis. Besides, finite difference approximated gradients may be very sensitive to the amplitude of ϵ, which makes such a method inappropriate for automatic shape optimization procedures (Haftka, 1985). Nevertheless this technique is commonly used to validate the $dq/d\alpha$ and $dJ/d\alpha$ values computed by the analytical methods.

3. Aeroelastic equilibrium

In the aeroelastic framework we have developped, fluid and structure are strongly coupled *i.e.* the static equilibrium is iteratively sought for till neither the aerodynamic nor the structural displacement fields evolve anymore. The flow problem is governed by the Euler equations. They are approximated by a second-order cell-centered finite volume scheme, and solved by a structured ONERA CFD solver elsA (Cambier *et al.*, 2008). The behavior of the structure is assumed to be linear and is predicted by beam theory. Even though this assumption may seem drastic, it has practical applications. In particular, beam theory predicts the deformation of high aspect-ratio wings and of helicopters blades with acceptable accuracy for design purposes. At the aeroelastic equilibrium, the set of Equations [6] is satisfied

$$\left\{ \begin{array}{l} R_a(W,X) = 0 \\ D - FL(W) = 0 \end{array} \right. \qquad [6]$$

where R_a is the set of discrete fluid equations, X is the vector of fluid grid nodes, F is the matrix of flexibility or influence coefficients matrix associated with the beam model, and L is the vector of aerodynamic loads applied on the beam.

From now on, we will assume that the structural mesh, denoted by Z, is composed of n_s nodes. The matrix of flexibility F is computed according to (Bisplinghoff *et al.*, 1996). This matrix depends on the spatial discretization of the structure. As a matter of fact, the coefficient $F_{l,m}$ represents the displacement of the beam mesh node l when a unitary load is applied on the beam mesh node m. In the framework we have developped, only the aerodynamic bending and torsion loads are transferred to the structure since they constitute the major contribution to the overall aerodynamic loads. Precisely, with the following system of coordinates (x, y, z) : x being aligned with the free stream flow, y being perpendicular to the aircraft symmetry plane, and z being pointing upwards, only the aerodynamic force F_z and the aerodynamic moments M_x and M_y are transferred to the structure. As a result, only the bending motion along z, denoted by ω_z, and the twist motion around y, denoted by θ_y and predicted by beam theory are used to remesh the fluid domain. In other words, the matrix of flexibility can be written as in Equation [7].

$$F = \left(\begin{array}{ccc} F^{\omega_z,F_z} & F^{\omega_z,M_x} & F^{\omega_z,M_y} \\ F^{\theta_y,F_z} & F^{\theta_y,M_x} & F^{\theta_y,M_y} \end{array} \right) \qquad [7]$$

For instance, F^{θ_y,M_x} is a (n_s, n_s) matrix and $F^{\theta_y,M_x}_{l,m}, 1 \leq l, m \leq n_s$, represents the angle of rotation θ_y around the y-axis induced at the structural mesh node l by a unit moment M_x around the x-axis applied on the structural mesh node m. So that the discrete structural equation is given by Equation [8].

$$(\omega_z \;\; \theta_y)^T = F \;\; (F_z \;\; M_x \;\; M_y)^T \qquad [8]$$

The coupled system of Equations [6] can be solved in one of two ways. The first way adopts the unique coupled system approach, and thus does not allow disciplines to proceed independently. Besides the two coupled physics are different, which often leads to ill-conditioned approximate jacobian matrices. The second way, which has been chosen in this study, uses the decomposition-into-coupled-subsystems approach : an integrated system solves the discipline separately and matches the solutions at the boundary interfaces. It consequently does not suffer from the aforementioned drawback. However, since the grid of the fluid domain and the mesh of the stuctural domain do not coincide at the coupling fluid/structure interface, two major difficulties have to be overcome. First, the aerodynamic loads, which are evaluated on the fluid mesh at the coupling interface, has to be transferred to the structural mesh. Second, the load-induced displacement field, which is calculated on the structural mesh, has to be transferred from the structural surface mesh to the fluid volumic grid. To do so, the fluid wet surface is divided into a number of slices equal to the number of beam mesh nodes, every beam node being located at the center of a slice.

3.1. *Fluid domain remeshing*

The structural displacements are responsible for the fluid domain to be deformed or in other words to be remeshed. The fluid computational domain is remeshed at every fluid-structure iteration towards the static aeroelastic equilibrium. The initial fluid grid X_{rig}, whose solid boundary belongs to the discrete parametrized shapes being optimized, is deformed analytically according to the structural displacements field D.

The analytical remeshing process is solid-mechanics inspired. More precisely, at each fluid-structure iteration, every grid node of the initial fluid grid X_{rig} is assigned a new location. If $N(i, j, k)$ designates a particular fluid grid node, N' its projection on the structural mesh, ω'_z and θ'_y respectively the bending and twist values linearly interpolated on the structural mesh and associated with N', then the new location of the grid node N results from the combination of the translational motion of vector ω'_z and the rotational motion through the angle θ'_y around the beam axis (the structural mesh being spread over this beam axis). This process is illustrated on Figure 1.

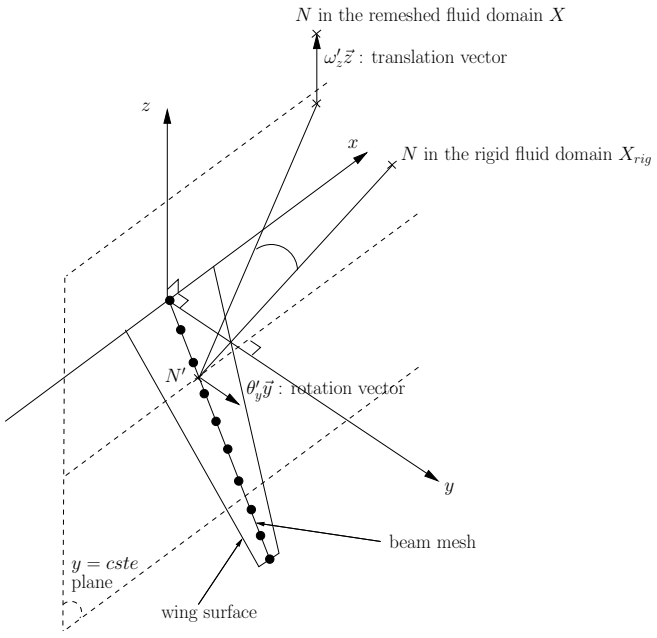

Figure 1. *Fluid domain remeshing process*

Explicitly, the $N(i,j,k)$ fluid grid node whose initial location in the X_{rig} grid is $(x_{rig}\ y_{rig}\ z_{rig})^T$, is assigned the new following location in the X grid :

$$\left(x(x_{rig}, y_{rig}, z_{rig}, \omega'_z, \theta'_y)\ \ y(x_{rig}, y_{rig}, z_{rig}, \omega'_z, \theta'_y)\ \ z(x_{rig}, y_{rig}, z_{rig}, \omega'_z, \theta'_y)\right)^T$$

We introduce the following variables : n_f designates the number of fluid interfaces of the wet coupling surface ; $Z = \{B_m,\ m \in [1, n_s]\}$ is the list of beam nodes forming the structural mesh ; S_l is the area of the fluid interface l, $l \in [1, n_f]$; O is the origin of the coordinate system ; and S_l^m is the area of the intersection of the fluid interface l and the slice m so that Equation [9] is satisfied.

$$\forall l \in [1, n_f] \qquad S_l = \sum_{m=1}^{n_s} S_l^m \qquad [9]$$

The new location of the fluid grid node $N(i,j,k)$ is then given by Equation [10], in which we have assumed that N', the projection of the fluid volumic grid node $N(i,j,k)$ on the wet surface, belongs to the slice l, and where ω_z^m and θ_y^m are respectively the bending and torsional displacement calculated at the structural mesh node B_m.

$$(x\ \ y\ \ z)^T = (x_{rig}\ \ y_{rig}\ \ z_{rig})^T + \sum_{m=1}^{n_s} \frac{S_l^m}{S_l} \left(\omega_z^m \vec{z} + \overrightarrow{NB_m} \wedge \theta_y^m \vec{y}\right) \qquad [10]$$

This relation is related to the prime notations according to Equation [11]. The new coordinates vector of the fluid computational domain X is a function of the coordinates vector of the initial fluid grid X_{rig} and of the displacements interpolated on the beam axis, which consequently depend on the displacements field computed on the structural mesh, D, and on the structural mesh coordinates, Z, so that $X(X_{rig}, Z, D)$.

$$\begin{cases} \sum_{m=1}^{n_s} \frac{S_l^m}{S_l} \omega_z^m \vec{z} = \omega_z' \vec{z} \\ \sum_{m=1}^{n_s} \frac{S_l^m}{S_l} \overrightarrow{NB_m} \wedge \theta_y^m \vec{y} = \overrightarrow{NN'} \wedge \theta_y' \vec{y} \end{cases} \quad [11]$$

$$=> (x \;\; y \;\; z)^T = (x_{rig} \;\; y_{rig} \;\; z_{rig})^T + \omega_z' \vec{z} + \overrightarrow{NN'} \wedge \theta_y' \vec{y}$$

3.2. *Aerodynamic loads transfer*

In order to guarantee an accurate aeroelastic equilibrium prediction, the load transfer has to be consistent and conservative (Maman *et al.*, 1995; Arian, 1997; Farhat *et al.*, 1998b; Farhat *et al.*, 1998a; Smith *et al.*, 2000).

We furthermore introduce the following variables : $\overrightarrow{\mathcal{F}_m}$ and $\overrightarrow{\mathcal{M}_m}$ are the aerodynamic force and moment transferred to the structural mesh node B_m ; G_l is the barycenter of the fluid interface l ; $\vec{n}_l$ is the unit normal vector of the fluid interface l and p_l is the static pressure on the fluid interface l, where $m \in [1, n_s]$ and $l \in [1, n_f]$.

$$\begin{cases} \overrightarrow{\mathcal{F}_m} = \sum_{l=1}^{n_f} S_l^m p_l \vec{n}_l \\ \overrightarrow{\mathcal{M}_m} = \overrightarrow{M}(B_m) = \sum_{l=1}^{n_f} \overrightarrow{B_m G_l} \wedge (S_l^m p_l \vec{n}_l) \end{cases} \quad [12]$$

The aerodynamic pressure load and moment transferred to the structural mesh node B_m is the sum of all the forces and moments applied on the slice m whose center is B_m. Using S_l^m to weigh the aerodynamic loads associated with the fluid interface l when evaluating the aerodynamic loads on the slice m enables the algorithm to sum over the whole set of fluid interfaces without making any distinction between those that do and those that do not intersect the slice l (since this weight is equal to zero when the interface is not included in the slice). Precisely, $\overrightarrow{\mathcal{F}_m}$ and $\overrightarrow{\mathcal{M}_m}$ are given by Equation [12].

$$\begin{cases} \overrightarrow{\mathcal{F}}_{\text{fluid surface}} = \sum_{l=1}^{n_f} S_l p_l \vec{n}_l \\ \overrightarrow{\mathcal{M}}_{\text{fluid surface}} = \sum_{l=1}^{n_f} \overrightarrow{OG_l} \wedge S_l p_l \vec{n}_l \end{cases} \quad [13]$$

This ensures the load transfer to be consistent (*i.e.* such that the total forces and moments transferred to the beam are the same as those evaluated on the grid surface). In fact, on one hand, the total aerodynamic force and moment, say at O, on the fluid surface mesh are given by Equation [13], and on the other hand, the total force and moment, still at O, transferred to the structural mesh are calculated according to Equations [14] and [15].

$$\overrightarrow{\mathcal{F}}_{\text{structural mesh}} = \sum_{m=1}^{n_s}\sum_{l=1}^{n_f} p_l S_l^m \vec{n}_l = \sum_{l=1}^{n_f}\left(\sum_{m=1}^{n_s} S_l^m\right) p_l \vec{n}_l = \sum_{l=1}^{n_f} p_l S_l \vec{n}_l \quad [14]$$

$$\begin{aligned}\overrightarrow{\mathcal{M}}_{\text{structural mesh}} &= \sum_{m=1}^{n_s}\left(\overrightarrow{\mathcal{M}_m} + \overrightarrow{OB_m}\wedge\overrightarrow{\mathcal{F}_m}\right)\\ &= \sum_{l=1}^{n_f}\sum_{m=1}^{n_s} S_l^m \overrightarrow{B_m G_l}\wedge p_l\vec{n}_l + \sum_{l=1}^{n_f}\sum_{m=1}^{n_s} S_l^m \overrightarrow{OB_m}\wedge p_l\vec{n}_l\\ &= \sum_{l=1}^{n_f}\left(\sum_{m=1}^{n_s} S_l^m\right)\overrightarrow{OG_l}\wedge p_l\vec{n}_l = \sum_{l=1}^{n_f}\overrightarrow{OG_l}\wedge p_l S_l\vec{n}_l\end{aligned} \quad [15]$$

The transfer is also conservative, *i.e.* the virtual work done by a virtual infinitesimal displacement of the structural mesh is the same as the virtual work done by the reported virtual infinitesimal displacement on the fluid surface. Any structural displacements field is reported on the volumic fluid grid according to Equation [10]. So that, the infinitesimal bending displacement, $\delta\omega_z^m$, and the infinitesimal torsion, $\delta\theta_y^m$, applied on the structural mesh node B_m induce the infinitesimal displacement $\overrightarrow{\delta\omega_l}$ on the barycenter of the fluid interface l (Equation [16]).

$$\overrightarrow{\delta\omega_l} = \sum_{m=1}^{n_s}\frac{S_l^m}{S_l}\delta\omega_z^m\vec{z} + \sum_{m=1}^{n_s}\frac{S_l^m}{S_l}\overrightarrow{G_l B_m}\wedge\delta\theta_y^m\vec{y} \quad [16]$$

The virtual work on the structural mesh and on the fluid surface mesh are respectively given by Equation [17] and Equation [18].

$$\begin{aligned}&\delta W_{\text{structural mesh}} = \sum_{m=1}^{n_s}\left(\overrightarrow{\mathcal{F}_m}\cdot\delta\omega_z^m\vec{z} + \overrightarrow{\mathcal{M}_m}\cdot\delta\theta_y^m\vec{y}\right) \quad =\\ &\sum_{m=1}^{n_s}\sum_{l=1}^{n_f}\left(\delta\omega_z^m S_l^m p_l\left(\vec{n}_l\cdot\vec{z}\right) + \left(\overrightarrow{B_m G_l}\wedge S_l^m p_l\vec{n}_l\right)\cdot\delta\theta_y^m\vec{y}\right)\end{aligned} \quad [17]$$

$$\begin{aligned}&\delta W_{\text{fluid surface}} = \sum_{l=1}^{n_f}\overrightarrow{\delta\omega_l}\cdot S_l p_l\vec{n}_l =\\ &\sum_{i=1}^{n_f}\sum_{m=1}^{n_s}\left(S_l^m\delta\omega_z^m\vec{z}\cdot p_l\vec{n}_l + S_l^m\left(\overrightarrow{G_l B_m}\wedge\delta\theta_y^m\vec{y}\right)\cdot p_l\vec{n}_l\right)\end{aligned} \quad [18]$$

Since Equation [19] is satisfied, it implies that $\delta W_{\text{beam mesh}} = \delta W_{\text{fluid surface}}$.

$$\left(\overrightarrow{G_l B_m} \wedge \delta\theta_y^m \vec{y}\right) \cdot p_l \vec{n}_l = \left(p_l \vec{n}_l \wedge \overrightarrow{G_l B_m}\right) \cdot \delta\theta_y^m \vec{y} = \left(\overrightarrow{B_m G_l} \wedge p_l \vec{n}_l\right) \cdot \delta\theta_y^m \vec{y} \quad [19]$$

3.3. *Iterative procedure towards the static aeroelastic equilibrium of the strongly coupled aeroelastic system*

This procedure is deliberately restricted to small displacement cases. So that, even though the structural mesh Z can depend on the design parameter vector α, *i.e.* not be a constant in the overall optimization process, it remains at its inital position Z_{rig} (depending on the design case being considered) during the fluid/structure iterations towards the static aeroelastic equilibrium.

The equilibrium solution of the coupled system is found by the following iterative fixed point procedure (the superscript (n) designates the n^{th} iteration) :

1) initialize the process by assuming $D^{(1)} = 0$ so that $X^{(1)} = X_{rig}$

2) compute the flow steady-state $W^{(n)}$ on the $X^{(n)}(X_{rig}, Z_{rig}, D^{(n)})$ fluid grid

3) compute and transfer the aerodynamic loads to the beam according to Equation [16]

4) compute its displacement $D^{(n+1)}$ and analytically deform X_{rig} according to Equation [16] to obtain $X^{(n+1)}(X_{rig}, Z_{rig}, D^{(n+1)})$

5) evaluate the new flow steady-state $W^{(n+1)}$

6) check convergence by inspecting the following criteria ϵ_a and ϵ_s are user-fixed tolerances)

$$\begin{cases} ||R_a||_2 \leq \epsilon_a \\ \\ ||D^{(n+1)} - D^{(n)}||_2 \leq \epsilon_s ||D^{(n)}||_2 \end{cases} \quad [20]$$

7) if the criteria are satisfied then stop the process, else go back to step 2.

4. Sensitivity analysis of the strongly coupled aeroelastic system

In the following, the vector of beam grid nodes is designated by Z and we consider the generic case for which J depends on the aerodynamic grid and field (X and W),

and on the structural grid and field (Z and D). The gradient of J with respect to α is then given by Equation [21].

$$\begin{aligned}\frac{dJ}{d\alpha} &= \frac{\partial J}{\partial \alpha} + \frac{\partial J}{\partial W}\frac{dW}{d\alpha} + \frac{\partial J}{\partial D}\frac{dD}{d\alpha} + \frac{\partial J}{\partial Z}\frac{dZ}{d\alpha} \\ &+ \frac{\partial J}{\partial X}\left(\frac{\partial X}{\partial X_{rig}}\frac{dX_{rig}}{d\alpha} + \frac{\partial X}{\partial Z_{rig}}\frac{dZ_{rig}}{d\alpha} + \frac{\partial X}{\partial D}\frac{dD}{d\alpha}\right)\end{aligned} \quad [21]$$

In this expression, the term between brakets represents the sensitivity of the remeshing process with respect to α. Since the new location of the grid nodes after every remeshing step is a function of the initial grid node locations X_{rig}, of the initial structural node locations Z_{rig} and of the structural displacement field D, the sensitivities of this three variables with respect to α have to be computed. The sensitivity of X_{rig} and Z_{rig} with respect to α is related to the optimization problem, more precisely to the design parameters being considered. On the contrary, the sensitivity of D with respect to α is not known a priori and has to be calculated. In the framework we have developped, all the derivatives appearing in the remeshing process related sensitivity term are computed analytically using the discrete formulation of the remeshing process, except $dX_{rig}/d\alpha$ and $dZ_{rig}/d\alpha$ which depend on the design problem and may be calculated using the approximative numerical finite difference technique.

4.1. *Discrete direct differentiation method*

If the direct differentiation method is to be used, one has to solve first for the sensitivities of the state variables W and D with respect to the design variables vector α. They are solutions of the system of Equations [22] obtained by differentiating Equation [6], where I denotes the identity matrix.

$$\left\{\begin{array}{l} \dfrac{\partial R_a}{\partial W}\dfrac{dW}{d\alpha} + \dfrac{\partial R_a}{\partial X}\dfrac{\partial X}{\partial D}\dfrac{dD}{d\alpha} = -\dfrac{\partial R_a}{\partial X}\dfrac{\partial X}{\partial X_{rig}}\dfrac{dX_{rig}}{d\alpha} - \dfrac{\partial R_a}{\partial X}\dfrac{\partial X}{\partial Z_{rig}}\dfrac{dZ_{rig}}{d\alpha} \\ \left(-F\dfrac{\partial L}{\partial W}\right)\dfrac{dW}{d\alpha} + \left(I - F\dfrac{\partial L}{\partial X}\dfrac{\partial X}{\partial D}\right)\dfrac{dD}{d\alpha} = \dfrac{dF}{d\alpha}L + F\dfrac{\partial L}{\partial X}\dfrac{\partial X}{\partial X_{rig}}\dfrac{dX_{rig}}{d\alpha} \\ \qquad + F\dfrac{\partial L}{\partial X}\dfrac{\partial X}{\partial Z_{rig}}\dfrac{dZ_{rig}}{d\alpha} + F\dfrac{\partial L}{\partial Z_{rig}}\dfrac{dZ_{rig}}{d\alpha} \end{array}\right. \quad [22]$$

The three terms $\partial L/\partial W$, $\partial L/\partial X$ and $\partial L/\partial Z_{rig}$ respectively represent the sensitivity of the aerodynamic loads transfering process with respect to the aerodynamic field above the wet surface, the fluid grid node coordinates and the structural mesh

node coordinates. In the framework we have developped, all these terms are derived analytically using the discrete formulation of the load transfer.

$$\left\{\begin{array}{l} \dfrac{\partial R_a}{\partial W}\dfrac{dW}{d\alpha_i}\Big|^{(n+1)} = -\dfrac{\partial R_a}{\partial X}\dfrac{\partial X}{\partial D}\dfrac{dD}{d\alpha_i}\Big|^{(n+1)} \\ \qquad -\dfrac{\partial R_a}{\partial X}\left(\dfrac{\partial X}{\partial X_{rig}}\dfrac{dX_{rig}}{d\alpha_i}+\dfrac{\partial X}{\partial Z_{rig}}\dfrac{dZ_{rig}}{d\alpha_i}\right) \\ \dfrac{dD}{d\alpha_i}\Big|^{(n+1)} = F\dfrac{\partial L}{\partial W}\dfrac{dW}{d\alpha_i}\Big|^{(n)} + F\dfrac{\partial L}{\partial X}\dfrac{\partial X}{\partial D}\dfrac{dD}{d\alpha_i}\Big|^{(n)} \\ \qquad + F\dfrac{\partial L}{\partial X}\left(\dfrac{\partial X}{\partial X_{rig}}\dfrac{dX_{rig}}{d\alpha_i}+\dfrac{\partial X}{\partial Z_{rig}}\dfrac{dZ_{rig}}{d\alpha_i}\right) + F\dfrac{\partial L}{\partial Z_{rig}}\dfrac{dZ_{rig}}{d\alpha_i} + \dfrac{dF}{d\alpha_i}L \end{array}\right. \quad [23]$$

In order to simplify the resolution and to make the implementation modular, an iterative process similar to the static aeroelastic computation process is used. It is inspired from the process described in (Martins, 2000; Martins *et al.*, 2004) and called "lagged" procedure. Namely, a discipline related sensitivity is calculated at the current iteration based on the other discipline sensitivity at the previous iteration. Moreover, to avoid the large matrix $F(\partial L/\partial X)(\partial X/\partial D)$ inversion, we have splitted the term multiplying $(dD/d\alpha_i)$ into $(dD/d\alpha_i)^{(n+1)}$, *i.e.* a term evaluated at the current solving iteration $n+1$, and a delayed term depending on $(dD/d\alpha_i)^{(n)}$, *i.e.* on a term already evaluated at the previous solving iteration n. The iterative procedure solving for Equation [22] is then doubly delayed : it contains a discipline-to-discipline delay similar to Martins' lagged procedure, as well as a related-to-structure only delay that we have introduced.

For every design parameter α_i, the linear system Equation [23] is solved iteratively (the superscript (n) designates the n^{th} iteration) :

1) initialize the process by assuming that $(dD/d\alpha_i)^{(1)} = 0$

2) compute the flow state sensitivity $(dW/d\alpha_i)^{(n)}$ based on $(dD/d\alpha_i)^{(n)}$

3) use $(dW/d\alpha_i)^{(n)}$ and $(dD/d\alpha_i)^{(n)}$ to compute $(dD/d\alpha_i)^{(n+1)}$

4) check convergence by inspecting the following criteria (ϵ_{da} and ϵ_{ds} are user-fixed tolerances)

$$\left|\left|\frac{dR_a}{d\alpha}\right|\right|_2 \leq \epsilon_{da} \quad \text{and} \quad \left|\left|\frac{dD}{d\alpha_i}\Big|^{(n+1)} - \frac{dD}{d\alpha_i}\Big|^{(n)}\right|\right|_2 \leq \epsilon_{ds}\left|\left|\frac{dD}{d\alpha_i}\Big|^{(n)}\right|\right|_2 \quad [24]$$

5) if the criteria are satisfied then stop the process, else go back to step 2.

The computation of the sensitivities of the n_f functions of interest with respect to the n_α considered design parameters (see Section 2), expected in particular by a gradient-based optimizer, requires either at least $n_\alpha + 1$ nonlinear system resolutions if the finite differencing method is used (with first-order formula), or one nonlinear system resolution (aeroelastic equilibrium calculation) added to n_α linear system resolutions (state variable gradients computation) if, on the contrary, the direct differentiation method is employed. In terms of CPU time, the iterative resolution of the linear System [22] is up to two times lower than the iterative resolution of the nonlinear System [6]. In terms of accuracy, since the direct differentiation method is an analytical method, it is reckoned to be also more precise.

4.2. *Discrete adjoint vector method*

If the discrete adjoint method is to be used, one has to solve the coupled system composed of Equations [25] and [26] where λ_a and λ_s are the adjoint vectors, associated with J, corresponding respectively to the aerodynamic and structure state equations.

$$\left(\frac{\partial R_a}{\partial W}\right)^T \lambda_a - \left(F\frac{\partial L}{\partial W}\right)^T \lambda_s = -\left(\frac{\partial J}{\partial W}\right)^T \quad [25]$$

$$\left(\frac{\partial R_a}{\partial X}\frac{\partial X}{\partial D}\right)^T \lambda_a + \left(I - F\frac{\partial L}{\partial X}\frac{\partial X}{\partial D}\right)^T \lambda_s = -\left(\frac{\partial J}{\partial X}\frac{\partial X}{\partial D} + \frac{\partial J}{\partial D}\right)^T \quad [26]$$

As in the direct differentiation method case, an iterative process is designed to simplify the resolution of the coupled system of Equations [25] and [26] and make its implementation modular, avoiding thus the inversion of a large sparse fluid/structure matrix.

$$\begin{cases} \left(\dfrac{\partial R_a}{\partial W}\right)^T \lambda_a\big|^{(n+1)} = \left(F\dfrac{\partial L}{\partial W}\right)^T \lambda_s\big|^{(n+1)} - \left(\dfrac{\partial J}{\partial W}\right)^T \\ \lambda_s\big|^{(n+1)} = \left(F\dfrac{\partial L}{\partial X}\dfrac{\partial X}{\partial D}\right)^T \lambda_s\big|^{(n)} - \left(\dfrac{\partial R_a}{\partial X}\dfrac{\partial X}{\partial D}\right)^T \lambda_a\big|^{(n)} \\ \qquad - \left(\dfrac{\partial J}{\partial X}\dfrac{\partial X}{\partial D} + \dfrac{\partial J}{\partial D}\right)^T \end{cases} \quad [27]$$

This process is embodied by Equation [27]. It is also in part inspired from the Martins' lagged procedure (Martins *et al.*, 2004). Namely, a discipline related adjoint vector is calculated at the current solving iteration based on the other discipline adjoint vector at the previous iteration. To avoid the large matrix $(F(\partial L/\partial X)(\partial X/\partial D))^T$ inversion, we have furthermore splitted the term multiplying λ_s into $\lambda_s|^{(n+1)}$, *i.e.* a term evaluated at the current solving iteration $n+1$, and a delayed term depending

on $\lambda_s\big|^{(n)}$, *i.e.* on a term already evaluated at the previous solving iteration n. The iterative procedure solving for the coupled system of Equations [25] and [26] is then doubly delayed : it contains a discipline-to-discipline delay similar to Martins' lagged procedure, as well as a related-to-structure only delay that we have introduced.

Precisely, every function to be differentiated requires the discrete adjoint linear system (Equation [27]) to be solved. This is achieved iteratively using the following process (the superscript (n) designates the n^{th} iteration) :

1) initialize the process by assuming that $\lambda_s\big|^{(1)} = 0$

2) compute the aerodynamic adjoint vector $\lambda_a\big|^{(n)}$ based on $\lambda_s\big|^{(n)}$

3) use $\lambda_a\big|^{(n)}$ and $\lambda_s\big|^{(n)}$ to compute $\lambda_s\big|^{(n+1)}$

4) check convergence by inspecting the following criteria (ϵ_{aa} and ϵ_{as} are user-fixed tolerances)

$$\begin{cases} \left|\left|\lambda_a\big|^{(n+1)} - \lambda_a\big|^{(n)}\right|\right|_2 \leq \epsilon_{aa}\left|\left|\lambda_a\big|^{(n)}\right|\right|_2 \\ \left|\left|\lambda_s\big|^{(n+1)} - \lambda_s\big|^{(n)}\right|\right|_2 \leq \epsilon_{as}\left|\left|\lambda_s\big|^{(n)}\right|\right|_2 \end{cases} \quad [28]$$

5) if the criteria are satisfied then stop the process, else go back to step 2.

The gradient of J is then given by Equation [29], once the adjoint vector λ_a and λ_s have been calculated they are plugged back in Equation [29] to access the sensitivity of J with respect to α.

$$\begin{aligned} \frac{dJ}{d\alpha} &= \frac{\partial J}{\partial \alpha} + \frac{\partial J}{\partial X}\frac{\partial X}{\partial X_{rig}}\frac{dX_{rig}}{d\alpha} + \frac{\partial J}{\partial X}\frac{\partial X}{\partial Z_{rig}}\frac{dZ_{rig}}{d\alpha} + \frac{\partial J}{\partial Z}\frac{dZ}{d\alpha} \\ &+ (\lambda_a)^T\left(\frac{\partial R_a}{\partial X}\frac{\partial X}{\partial X_{rig}}\frac{dX_{rig}}{d\alpha} + \frac{\partial R_a}{\partial X}\frac{\partial X}{\partial Z_{rig}}\frac{dZ_{rig}}{d\alpha}\right) \\ &- (\lambda_s)^T\left(\frac{dF}{d\alpha}L + F\frac{\partial L}{\partial X}\frac{\partial X}{\partial X_{rig}}\frac{dX_{rig}}{d\alpha} + F\frac{\partial L}{\partial X}\frac{\partial X}{\partial Z_{rig}}\frac{dZ_{rig}}{d\alpha}\right) \\ &- (\lambda_s)^T\left(F\frac{\partial L}{\partial Z_{rig}}\frac{dZ_{rig}}{d\alpha}\right) \end{aligned} \quad [29]$$

The computation of the sensitivities of the n_f functions of interest with respect to the n_α considered design parameters (see Section 2), expected in particular by a gradient-based optimizer, requires either at least $n_\alpha + 1$ nonlinear system resolutions if the finite differencing method is used (with first-order formula), or one nonlinear system resolution (aeroelastic equilibrium calculation) added to n_f linear system

resolutions (adjoint vectors computation) if, on the contrary, the adjoint method is employed. In terms of CPU time, the iterative resolution of the linear system composed of Equations [25] and [26] can be up to three times higher than the iterative resolution of the nonlinear System [6]. However, since in common shape optimization problems, the number of functions of interest (tens or so) is far less than the number of design parameters (hundreds or so), evaluating their gradients with the adjoint method is faster than using a finite differencing method. In terms of accuracy, the adjoint method being an analytical method, it is expected to be also more accurate.

Solving the discrete direct and adjoint systems arises two major difficulties. First, one has to transfer data back and forth between the two separate subsytems. Second, the computation of the partial derivatives terms, in particular the cross discipline terms, is particularly laborious. For instance, if one wishes to compute the sensitivity of the aerodynamic loads transferred to the beam with respect to the aerodynamic grid coordinates ($\partial L/\partial X$), one has first to compute the sensitivities of these loads with respect to the boundary surface and to the boundary flow variables, and then to compute the sensitivity of the boundary surface and of the boundary flow variables with respect to each aerodynamic grid node coordinate.

In the present work, every terms appearing in Equation [23] and Equation [27] are calculated analytically, except the terms $(\partial R_a/\partial X * dX/d\alpha_i)$ and $(\partial R_a/\partial X * \partial X/\partial D)$, which are numerically evaluated (central finite differences). The aerodynamic subsystem is solved by a Newton-like method with an approximate jacobian. At each Newton-like iteration the linearized problem is solved by a LU relaxation method (Peter, 2006).

5. Applications

Here, we apply the coupled direct and adjoint methods to the sensitivity analysis of the DLR F4 wing-body configuration (Redeker *et al.*, 1983). First, the static aeroelastic analysis is described, then the analytical sensitivity derivatives are compared to the finite difference values for three different design parameters. The aircraft is assumed to fly in symmetric cruise conditions. Consequently, only the flow around the right part of the F4 wing-body configuration is considered. The flow is governed by the Euler equations, the fluid computational domain (scale model dimensions) is covered with a multiblock mesh composed of $313,650$ nodes. Besides, only the wing is supposed to deform due to aerodynamic loads. The fuselage remains rigid while a beam mesh is defined to simulate the aeroelastic displacement of the wing. The free-stream conditions are summarized in Table 1. In particular, three free-stream angle of attack (aoa) have been considered.

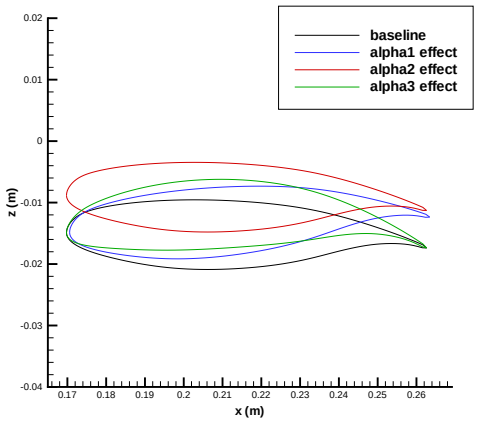

Figure 2. *Positive α_1, α_2 and α_3-induced variations of the wing cross-section (at mid-span)*

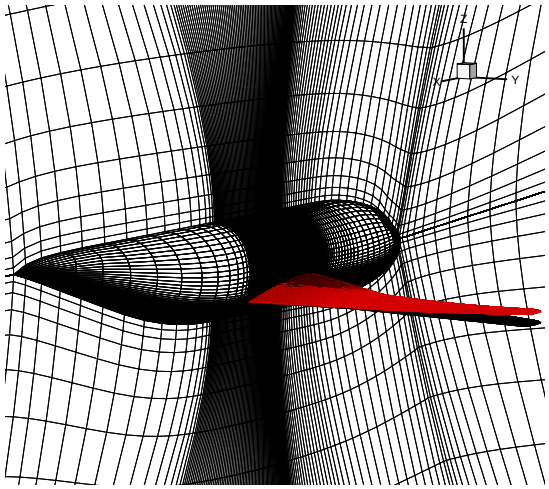

Figure 3. *Aircraft static aeroelastic position (upper) versus jig-shape position (lower) (0.93° aoa)*

The beam geometry is discretized by 250 nodes and its structural characteristics are reported in Table 2, they have been deduced from the experimental aeroelastic displacements data available for the European project HiReTT wing-fuselage configuration (Braun *et al.*, 2003). For each beam section, the quadratic momentums I and

J, respectively related to the bending and torsional structural motion, are analytically calculated based on the wing cross section geometries assuming solid body structure made of isotropic material (aluminium).

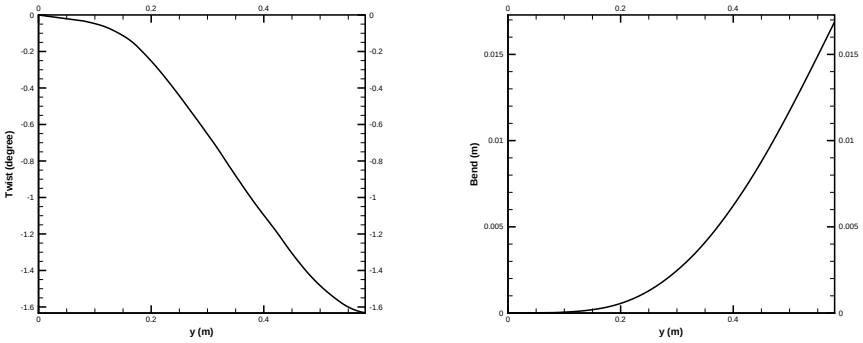

(a) Beamwise twist.

(b) Beamwise bending deflection.

Figure 4. *Beam displacement at the static aeroelastic equilibrium (*0.93° *aoa)*

Table 1. *Cruise flight conditions*

Angle of attack	-1° ,0.93°,3°
Free-stream density	$9.015 \quad kg/m^3$
Free-stream static pressure	$6.977 \cdot 10^4 \quad N/m^2$
Free-stream Mach number	0.75

Table 2. *Beam material characteristics*

Young's modulus	$E = 1.813 \cdot 10^{11} \quad N/m^2$
Shear modulus	$G = 0.682 \cdot 10^{11} \quad N/m^2$
Poisson's ratio	$\nu = 0.33$

The equilibrium position of the swecond flight condition is reached after about six fluid-structure coupling iterations (cf. Figure 3 and Figure 4) : the iterative process described in Section 3.3 is then converged with $\epsilon_a = 10^{-3}$ and $\epsilon_s = 10^{-4}$. The rate of convergence of the aeroelastic system depends on the angle of attack of the free stream. This is illustrated by Figure 6 which shows the rates of convergence of the

square norm of the aerodynamic equations residual over the global fluid/structure iterative process solving for the static aeroelastic equilibrium for the three different free-stream angles of attack that have been considered. Similarly, the structural displacement field is convergent (cf. Figure 10), it reaches a constant value at the end of the fluid/structure iterative process. The static aeroelastic position of the aircraft is in fact the so called 1-g shape which has been recovered by the aeroelastic iterative process starting with the rigid jig-shape of the aircraft.

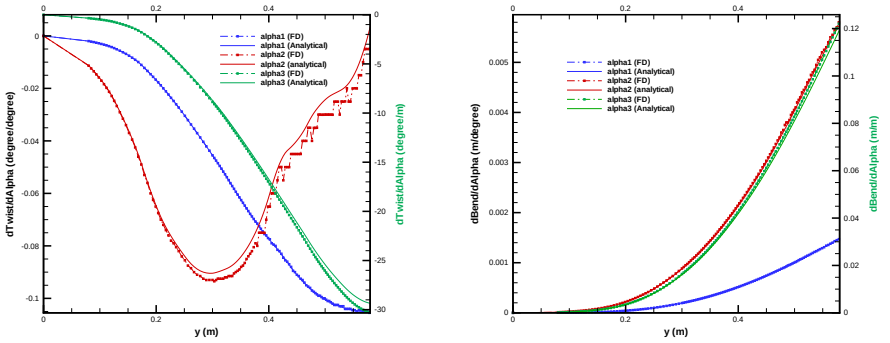

(a) Beamwise twist sensitivity.

(b) Beamwise bending deflection sensitivity.

Figure 5. *Beam displacement sensitivities wrt* α_1, α_2, *and* α_3 *(*$0.93°$ *aoa)*

The effects of three design parameters on the aerodynamic lift and drag coefficients, respectively denoted by C_l and C_d, are computed (Destarac, 2003). The first parameter (α_1) modifies the built-in spanwise twist law of the wing, the second parameter (α_2) introduces a spanwise bump along the wing, and the third parameter (α_3) introduces a linear variation of the airfoil maximum camber along the span (cf. Figure 2). These parameters do not affect the structural characteristics of the wing so that $dF/d\alpha = 0$ and $dZ/d\alpha = 0$. A series of decreasing steps have been tested during the finite difference derivatives computation process, so that the values reported on the graphs and in the tables can be considered as converged.

The direct method actually solves for the beam displacements derivatives and the conservative flow state variables derivatives, from which the pressure coefficient derivatives can be deduced straightforwardly. These derivatives are shown in Figure 5 and 9. They compare very well with the finite difference respective sensitivities.

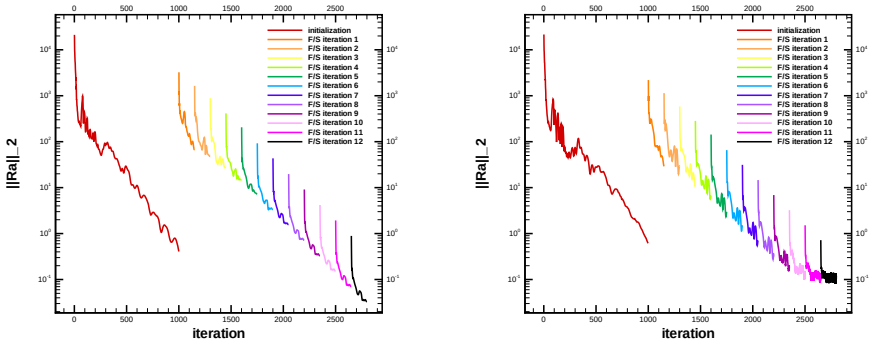

(a) 0.93° aoa. (b) -1° aoa.

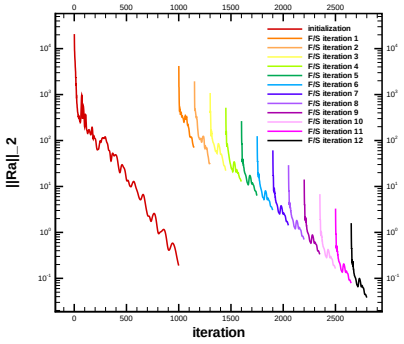

(c) 3° aoa.

Figure 6. *Residual convergence over the fluid/structure iterative process*

The derivatives of C_l and C_d have been computed by the methods described in this paper and are summarized in Tables 3, 4 and 5. In cruise conditions (0.93° aoa), an increase in the wing built-in twist or in the wing camber law augments the outer wing loading, which increases the lift coefficient as well as the drag coefficient due in particular to a rise in the induced drag. This also results, due to aeroelastic coupling, in an increase of the wing deflection and a decrease of the wing twist due to the stabilizing bending-twist geometrical coupling of backward swept wings.

Table 3. *The sensitivity derivatives of the drag and lift coeffi cients (0.93° aoa)*

$\mathbf{dC_d/d\alpha_1}$	$\mathbf{dC_d/d\alpha_2}$	$\mathbf{dC_d/d\alpha_3}$	$\mathbf{dC_l/d\alpha_1}$	$\mathbf{dC_l/d\alpha_2}$	$\mathbf{dC_l/d\alpha_3}$
Direct differentiation method (DDM) :					
$3.146\ 10^{-3}$	0.03187	0.1215	0.03966	0.3587	3.0457
Adjoint vector method (AVM) :					
$3.142\ 10^{-3}$	0.03189	0.1207	0.03967	0.3585	3.0452
Finite difference method (FD) :					
$3.138\ 10^{-3}$	0.03183	0.1201	0.03962	0.3591	3.0601
AVM vs DDM :					
0%	0%	0%	0%	0%	0%
DDM vs FD :					
0.3%	0%	0%	0%	0.2%	0.6%
AVM vs FD :					
0.3%	0%	0%	0%	0.2%	0.6%

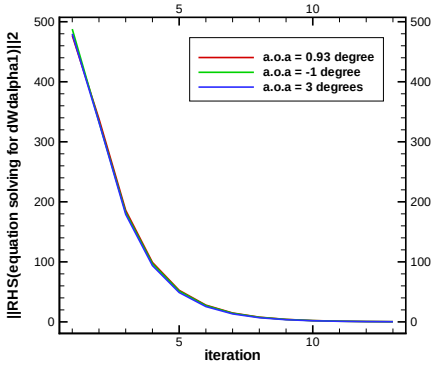

Figure 7. *Convergence of the square norm of the right hand side (rhs) of the equation [22] solving for $dW/d\alpha_1$ (associated with the fi rst fluid state variable) over the fluid/structure iterative process for 3 aoa*

The iterative process used to solve the coupled discrete direct and discrete adjoint systems needs generally few iterations to converge. In fact, the process described in Section 4.1 requires six iterations to converge with $\epsilon_{da} = 10^{-3}$ and $\epsilon_{ds} = 10^{-4}$.

Table 4. *The sensitivity derivatives of the drag and lift coeffi cients (−1° aoa)*

$\mathbf{dC_d/d\alpha_1}$	$\mathbf{dC_d/d\alpha_2}$	$\mathbf{dC_d/d\alpha_3}$	$\mathbf{dC_l/d\alpha_1}$	$\mathbf{dC_l/d\alpha_2}$	$\mathbf{dC_l/d\alpha_3}$
Direct differentiation method (DDM) :					
$-7.795\ 10^{-4}$	0.012017	0.1027	−0.0298	0.2166	2.9345
Adjoint vector method (AVM) :					
$-7.797\ 10^{-4}$	0.012013	0.1019	−0.0297	0.2167	2.9343
Finite difference method (FD) :					
$-7.786\ 10^{-4}$	0.012005	0.1013	−0.0290	0.2152	2.9502
AVM vs DDM :					
0%	0%	0%	0%	0%	0%
DDM vs FD :					
0.1%	0%	0%	0%	0.4%	0.6%
AVM vs FD :					
0.1%	0%	0%	0%	0.4%	0.6%

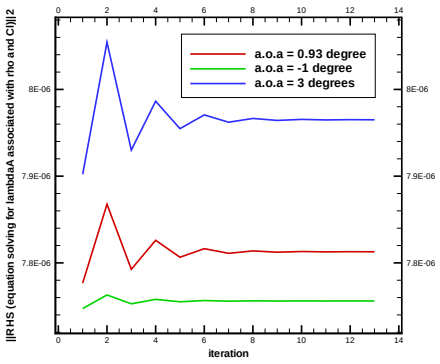

Figure 8. *Convergence of the square norm of the rhs of the equation [25] solving for λ_a (associated with the fi rst fluid state equation) over the fluid/structure iterative process for 3 aoa*

Similarly, after six data transfers between the fluid solver and the structure solver, the iterative process conceived to solve the coupled discrete direct differentiation system described in Section 4.2 is converged with $\epsilon_{da} = 10^{-5}$ and $\epsilon_{ds} = 10^{-4}$ (using Equation [28] notations). To illustrate this convergence, the square norms of the right

hand side of Equation [22], solving for $dW/d\alpha$, and of Equation [25], solving for λ_a, over the iterative solving process have been reported on Figures 7 and 8. Since, they converge to constant values, it indicates that their solutions $dW/d\alpha$ and λ_a behave the same.

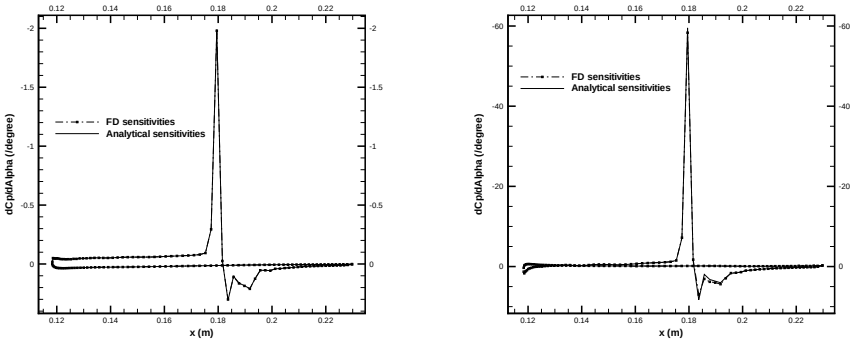

(a) Wrt α_1.

(b) Wrt α_2.

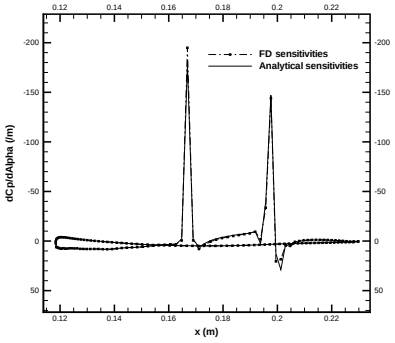

(c) Wrt α_3.

Figure 9. *C_p sensitivity on the wing cross-section at mid-span (discrete direct differentiation method) (0.93° aoa)*

Likewise, the rates of convergence of $dD/d\alpha_1$ (direct method) and of λ_s (adjoint method) associated with each displacement equation, namely the twist and the bending equations, and corresponding to the two functions that have been considered, namely C_l and C_d, at wing tip are described by Figures 11 and 12.

Table 5. *The sensitivity derivatives of the drag and lift coeffi cients (3° aoa)*

$dC_d/d\alpha_1$	$dC_d/d\alpha_2$	$dC_d/d\alpha_3$	$dC_l/d\alpha_1$	$dC_l/d\alpha_2$	$dC_l/d\alpha_3$
Direct differentiation method (DDM) :					
$-3.668\ 10^{-3}$	0.039775	0.1033	−0.0287	0.3514	2.7559
Adjoint vector method (AVM) :					
$-3.667\ 10^{-3}$	0.039769	0.1029	−0.0285	0.3512	2.7553
Finite difference method (FD) :					
$-3.713\ 10^{-3}$	0.039821	0.1041	−0.0288	0.3530	2.7609
AVM vs DDM :					
0%	0%	0%	0%	0%	0%
DDM vs FD :					
2%	0.3%	0%	0%	0.5%	0.4%
AVM vs FD :					
2%	0.3%	0%	0%	0.5%	0.4%

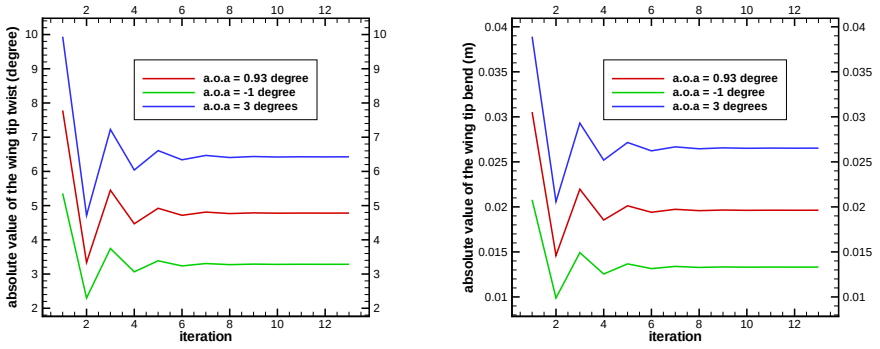

(a) Twist.

(b) Bending deflection.

Figure 10. *Wing tip displacement convergence over the fluid/structure iterative process for 3 aoa*

The analytical results compare very well with the finite difference values (cf. Tables 3, 4 and 5), which, given the coding complexity of these techniques, proves the successful implementation of the analytical methods and opens up the possibility of

using analytical gradients in the shape optimization process of fluid-structure coupled systems, whose advantages with respect to the finite difference values in terms of accuracy and computational time saving are obvious. Besides, the present work shows that not taking fluid-structure interaction into account leads to significantly different results. In fact, using the pure aerodynamic approach to compute the aerodynamic coefficients sensitivities can cause the values to be up to 50% different from those calculated using the aeroelastic approach (cf. Table 6).

Table 6. *The sensitivities of the drag and lift aerodynamic coeffi cients computed with and without taking fluid-structure interactions into account*

$\mathbf{dC_d/d\alpha_1}$	$\mathbf{dC_d/d\alpha_2}$	$\mathbf{dC_d/d\alpha_3}$	$\mathbf{dC_l/d\alpha_1}$	$\mathbf{dC_l/d\alpha_2}$	$\mathbf{dC_l/d\alpha_3}$
No coupling :					
$2.341\ 10^{-3}$	$3.788\ 10^{-2}$	0.1802	0.0402	0.3271	4.2532
F/S coupling :					
$3.149\ 10^{-3}$	$3.189\ 10^{-2}$	0.1224	0.0396	0.3584	3.0403
Relative difference :					
25%	19%	50%	1.5%	9%	40%

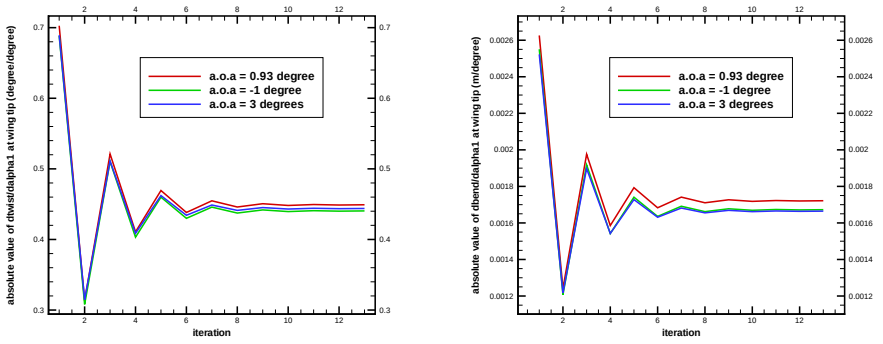

(a) Twist sensitivity.

(b) Bending deflection sensitivity.

Figure 11. *Convergence of beam displacement sensitivity at wing tip wrt α_1 over the fluid/structure iterative process for 3 aoa*

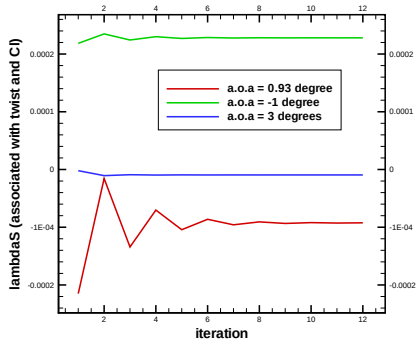

(a) Corresponding to C_l and associated with twist

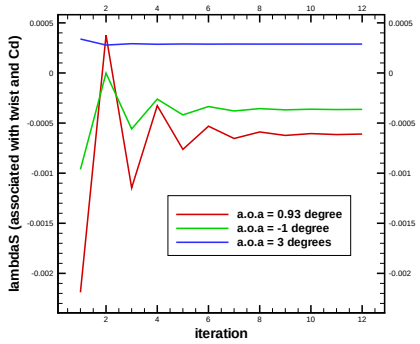

(b) Corresponding to C_d and associated with twist

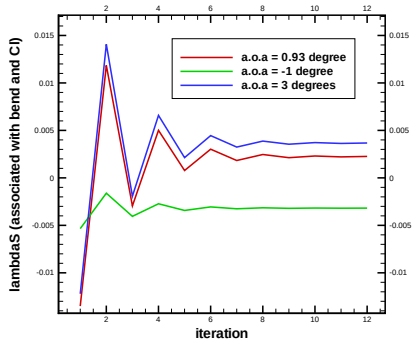

(c) Corresponding to C_l and associated with bending

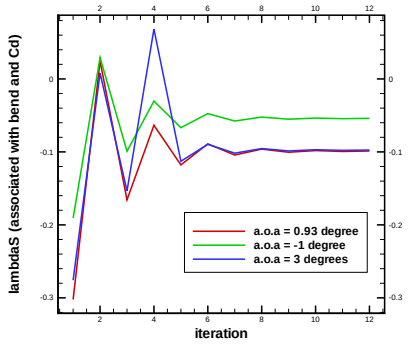

(d) Corresponding to C_d and associated with bending

Figure 12. *Convergence of the adjoint structural vectors over the fluid/structure iterative process for 3 aoa at wing tip*

6. Conclusions

A computational framework for the sensitivity analysis of an steady nonlinear aeroelastic system has been described. The aeroelastic state is predicted based on beam theory and Euler equations, and the sensitivities of the coupled system can be analytically computed either by the discrete direct or the discrete adjoint method. Such a framework has never been presented before, however it is particularly well-

adapted to preliminary design phases enabling the designer to take fluid-structure coupling into account from the first design phase. The aeroelastic analysis and the sensitivity derivatives calculation rely on two different lagged algorithms, whose solutions are the conservative flow state variables and the structural displacements at the aeroelastic equilibrium and either the state variables derivatives or the adjoint vectors. The proposed methodology has been applied to the sensitivity analysis of the flexible DLR F4 wing-body configuration with respect to three design parameters using both the coupled discrete direct differentiation and coupled discrete adjoint methods. This application has proved the accuracy and the computational efficiency of the analytical analyses. Future studies will include the extension of the proposed methodology to Reynolds Average Navier-Stokes equations for evaluating the fluid variables and to finite-element model for predicting the structural displacement field.

7. References

Arian E., « On the Coupling of Aerodynamic and Structural Design », *Journal of Computational Physics*, vol. 135, n° 1, p. 83-96, 1997.

Arslan A., Carlson L., « Integrated Determination of Sensitivity Derivatives for an Aeroelastic Transonic Wing », *Journal of Aircraft*, vol. 33, n° 1, p. 224-231, 1996.

Barthelemy J.-F., Wrenn G., Dovi A., Hall L., « Supersonic Transport Wing Minimum Weight Design Integrating Aerodynamics and Structures », *AIAA Journal of Aircraft*, vol. 31, n° 2, p. 330-338, 1994.

Baysal O., Eleshaky M., « Aerodynamic Design Sensitivity Analysis Methods for the Compressible Euler Equations », *Journal of Fluids Engineering*, vol. 113, n° 4, p. 681-688, 1991.

Bendsoe M., *Optimization of Structural Topology, Shape, and Material*, Springer Verlag, New York, USA, 1995.

Bisplinghoff R., Ashley H., Halfman R., *Aeroelasticity*, Dover Science Books, New York, USA, 1996.

Bowman K., Grandhi R., Eastep F., « Optimum Design of Lifting Surfaces with Aeroelastic Divergence and Control Reversal Considerations », *International Journal for Structural Optimization*, vol. 1, p. 153-161, 1989.

Braun C., Boucke A., Ballmann J., Hanke M., Karavas A., Numerical Prediction of the Model Deformation of a High Speed Transport Aircraft Type Wing by Direct Aeroelastic Simulation, Technical Report n° HIRETT/TR/RWTH/CB/18032003/1, Rheinisch-Westfalische Technische Hochschule Aachen Lehr-und Forschungsgebiet fur Mechanik, 2003.

Burgreen G., Baysal O., « Three-dimensional Aerodynamic Shape Optimization Using Discrete Sensitivity Analysis », *AIAA Journal*, vol. 34, p. 1761-1770, 1996.

Cambier L., Veuillot J., « Status of the elsA CFD Software for Flow Simulation and Multidisciplinary Applications », *in Proceedings of the 46th AIAA Aerospace Science Meeting and Exhibit, AIAA Paper 2008-664*, Reno, USA, 2008.

Carrier G., « Multidisciplinary Optimization of a Supersonic Transport Aircraft Wing Planform », *in Proceedings of the European Congress on Computational Methods in Applied Sciences and Engineering ECCCOMAS 2004*, Jyvaskyla, Sweden, juillet, 2004.

Carrier G., « Single and Multi-Point Aerodynamic Optimizations of a Supersonic Transport Aircraft Wing Using Optimization Strategies Involving Adjoint Method and Genetic Algorithm », *in Proceedings of ERCOFTAC*, Las Palmas, Spain, avril, 2006.

Destarac D., « Far-Field / Near-Field Drag Balance and Applications of Drag Extraction in CFD », *VKI Lecture Series 2003, CFD-based Aircraft Drag Prediction and Reduction, National Institute of Aerospace, Hampton (VA)*, 2003.

Din I. S. E., Carrier G., Mouton S., « Discrete adjoint method in elsA (Part II) : application to aerodynamic design optimization », *in Proceedings of the 7th ONERA-DLR Aerospace Symposium*, Toulouse, France, 2006.

Farhat C., Lesoinne M., LeTallec P., « Conservative Algorithm for Exchanging Aerodynamic and Elastodynamic Data in Aeroelastic Systems », *in Proceedings of the 36th AIAA Aerospace Science Meeting and Exhibit, AIAA Paper 1998-16371*, Reno, USA, 1998a.

Farhat C., Lesoinne M., LeTallec P., « Load and Motion Transfer Algorithms for Fluid/Structure Interaction Problems with Non-matching Discrete Interfaces : Momentum and Energy Conservation, Optimal Discretization and Application to Aeroelasticity », *Computer Methods in Applied Mechanics and Engineering*, vol. 157, n° 1, p. 95-114, 1998b.

Fazzolari A., Gauger N., Brezillon J., « Efficient aerodynamic shape optimization in MDO context », *Journal of Computational and Applied Mathematics*, vol. 203, n° 2, p. 548-560, 2007.

Fillola G., LePape M.-C., Montagnac M., « Numerical Simulations Around Wing Control Surfaces », *in Proceedings of the 24th International Congress of the Aeronautical Sciences, ICAS 2004*, Yokohama, Japan, 2004.

Friedman P., « Helicopter Vibration Reduction Using Structural Optimization with Aeroelastic/Multidisciplinary Constraints - a Survey », *Journal of Aircraft*, vol. 28, n° 1, p. 8-21, 1991.

Ghattas O., Li X., « Domain Decomposition Methods for Sensitivity Analysis of a Nonlinear Aeroelastic Problem », *International Journal of Computational Fluid Dynamics*, vol. 11, p. 113-130, 1998.

Giunta A., « A Novel Sensitivity Analysis Method for High-Fidelity Multidisciplinary Optimization of Aero-Structural Systems », *in Proceedings of the 38th AIAA Aerospace Science Meeting and Exhibit, AIAA Paper 2000-683*, Reno, USA, 2000.

Giunta A., Sobieszcsanski-Sobieski J., « Progress Toward Using Sensitivity Derivatives in a High-Fidelity Aeroelastic Analysis of a Supersonic Transport », *in Proceedings of the 7th AIAA/USAF/NASA/ISSMO Symposium on Multidisciplinary Analysis and Design, AIAA Paper 1998-4763*, 1998.

Haftka R., « Sensitivity calculations for Iteratively Solved Problems », *International journal of numerical methods in engineering*, vol. 21, p. 1535-1546, 1985.

Haftka R., « Structural Optimization with Aeroelastic Constraints - a Survey of U.S. Applications », *International Journal of Vehicle Design*, vol. 7, p. 381-392, 1986.

Haug E., Choi K., Komkov V., *Design Sensitivity Analysis of Structural Systems*, Academic Press, Orlando, USA, 1986.

Hicks R., Henne P., « Wing Design by Numerical Optimization », *Journal of Aircraft*, vol. 15, n° 7, p. 407-412, 1978.

Hicks R., Murman E., Vanderplaats G., An Assesment of Airfoil Design by Numerical Optimization, Technical Report n° TMX 3092, NASA, 1976a.

Hicks R., Vanderplaats G., « Design of Low-Speed Airfoil by Numerical Optimization », *SAE*, 1975.

Hicks R., Vanderplaats G., « Airfoil Section Drag Reduction at Transonic Speeds by Numerical Optimization », *SAE*, 1976b.

Hicks R., Vanderplaats G., « Application of Numerical Optimization to the Design of Supercritical Airfoil Without Drag Creep », *SAE*, 1977.

Hou G., Satyanarayana A., « Analytical Sensitivity Analysis of a Static Aeroelastic Wing », *in Proceedings of the AIAA/USAF/NASA/ISSMO Symposium on Multidisciplinary Analysis and Optimization, AIAA Paper 2000-4824*, Long Beach, USA, septembre, 2000.

Jameson A., « Aerodynamic Design Via Control Theory », *Journal of Scientific Computing*, vol. 3, n° 3, p. 233-260, 1988.

Jameson A., « Automatic Design of Transonic Airfoils to Reduce the Shock Induced Pressure Drag », *in Proceedings of the 31th Israel Annual Conference on Aviation and Aeronautics*, Tel-Aviv, Israel, février, 1990.

Jameson A., Pierce N., Martinelli L., « Optimum Aerodynamic Design Using the Navier-Stokes Equations », *Theoretical and computational fluid dynamics*, vol. 10, p. 213-237, 1998.

Jameson A., Reuther J., « Control Theory Based Airfoil Design Using the Euler Equations », *in Proceedings of the 5th AIAA/USAF/NASA/ISSMO Symposium on Multidisciplinary Analysis and Optimization, AIAA Paper 1994-4272*, Panama City Beach, USA, septembre, 1994.

Kirsch U., *Structural Optimization : Fundamentals and Applications*, Springer Verlag, New York, USA, 1993.

Lions J.-L., *Optimal Control of Systems Governed by Partial Differential Equations*, Springer Verlag, New York, USA, 1971.

Maman N., Farhat C., « Matching Fluid and Structure Meshes for Aeroelastic Computations : a Parallel Approach », *Computers & Structures*, vol. 54, n° 4, p. 779-784, 1995.

Martins J., A coupled-adjoint Method for High-fidelity Aero-structural Optimization, PhD thesis, Stanford University (CA), 2000.

Martins J., Alonso J., Reuther J., « High-Fidelity Aerostructural Design Optimization of a Supersonic Businees Jet », *Journal of Aircraft*, vol. 41, n° 3, p. 523-530, 2004.

Maute K., Nikbay M., Farhat C., « Coupled Analytical Sensitivity Analysis and Optimization of Three-Dimensional Nonlinear Aeroelastic Systems », *AIAA Journal*, vol. 39, n° 11, p. 2051-2061, 2001.

Maute K., Nikbay M., Farhat C., « Sensitivity Analysis and Design Optimization of Three-Dimensional Nonlinear Aeroelastic Systems by the Adjoint Method », *International Journal for Numerical Methods in Engineering*, vol. 56, n° 6, p. 911-933, 2003.

Moller H., Lund E., « Shape Sensitivity Analysis of Strongly Coupled Fluid-Structure Interaction Problems », *in Proceedings of the 43rd AIAA/ASME/ASCE/AHS/ASC Structures, Structural Dynamics and Materials Conference, AIAA Paper 2002-1478*, Denver, USA, 2002.

Peter J., « Discrete Adjoint Method in elsA (Part I) : Method/Theory », *in Proceedings of the 7th ONERA-DLR Aerospace Symposium*, Toulouse, France, 2006.

Pironneau O., « On Optimal Shapes for Stokes Flow », *Journal of Fluid Mechanics*, vol. 70, n° 2, p. 117-128, 1973.

Redeker G., Muller R., A Comparison of Experimental Results for the Transonic Flow Around the DFVLR-F4 Wing-Body Configuration, Technical Report n° GARTEUR-TP018, DLR-IB 129 -83/21, DLR, 1983.

Reuther J., Aerodynamic Shape Optimization Using Control Theory, PhD thesis, University of California Davis, 1996.

Reuther J., Jameson A., Alonso J., Rimlinger M., Saunders D., « Constrained Multipoint Aerodynamic Shape Optimization Using an Adjoint Formulation and Parallel Computers, Part I », *Journal of Aircraft*, vol. 36, n° 1, p. 51-60, 1999a.

Reuther J., Jameson A., Alonso J., Rimlinger M., Saunders D., « Constrained Multipoint Aerodynamic Shape Optimization Using an Adjoint Formulation and Parallel Computers, Part II », *Journal of Aircraft*, vol. 36, n° 1, p. 61-74, 1999b.

Reuther J., Jameson A., Farmer J., Martinelli L., Saunders D., « Aerodynamic Shape Optimization of Complex Aircraft Configurations via an Adjoint Formulation », *in Proceedings of the 34th AIAA Aerospace Science Meeting and Exhibit, AIAA Paper 96-0094*, Reno, USA, 1996.

Shubin G., Obtaining Cheap Optimization Gradients from Computational Aerodynamics Codes, Technical Report n° Tech. Rep. AMS-TR-164, Boeing Computer Service, Applied Mathematics and Statistics, 1991.

Shubin G., Frank P., A Comparison of Implicit Gradient Approach and the Variational Approach to Aerodynamic Design Optimization, Technical Report n° Tech. Rep. AMS-TR-163, Boeing Computer Service, Applied Mathematics and Statistics, 1991.

Smith M., Hodges D., Cesnik C., « Evaluation of Computational Algorithms Suitable for Fluid-Structure Interactions », *Journal of Aircraft*, vol. 37, n° 2, p. 282-294, 2000.

Sobieszcsanski-Sobieski J., « Sensitivity Analysis and Multidisciplinary Optimization for Aircraft Design : Recent Advances and Results », *Journal of Aircraft*, vol. 27, n° 12, p. 993-1001, 1990a.

Sobieszcsanski-Sobieski J., « Sensitivity of Complex, Internally Coupled Systems », *AIAA Journal*, vol. 28, n° 1, p. 153-160, 1990b.

Vanderplaats G., *Numerical Optimization Techniques for Engineering Design : with Applications*, McGraw-Hill, New York, USA, 1984.

Vanderplaats G., Hicks R., Numerical Airfoil Optimization Using a Reduced Number of Design Coordinates, Technical Report n° Technical Report TMX 73151, NASA, 1976.

Wakayama S., Lifting Surface Design Using Multidisciplinary Optimization, PhD thesis, Stanford University (CA), 1994.

Article reçu le 28 février 2008
Accepté après révisions le 11 septembre 2008